

# Infall and SiO emission in V838 Mon

M. T. Rushton<sup>1</sup>, T. R. Geballe<sup>2</sup>, A. Evans<sup>1</sup>, B. Smalley<sup>1</sup>, J. Th. van Loon<sup>1</sup>,  
S. P. S. Eyres<sup>3</sup>

<sup>1</sup> *Astrophysics Group, School of Physical and Geographical Sciences, Keele University, Keele, Staffordshire, ST5 5BG, UK*

<sup>2</sup> *Gemini Observatory, 670 N. A‘ohōkū Place, University Park, Hilo, HI 96720, USA*

<sup>3</sup> *Centre for Astrophysics, University of Central Lancashire, Preston, PR1 2HE, UK*

Version of 22 Oct 2004

## ABSTRACT

We present moderate and high resolution infrared spectroscopy of the peculiar eruptive variable V838 Mon, which underwent a series of remarkable outbursts in early 2002. During the period covered by our observations, 2002 December–2003 December, the near-infrared spectrum continued to show many of the characteristics of a very cool supergiant. However, throughout this period the spectrum also revealed strong and variable SiO first overtone emission, and Pa $\beta$  emission. The 2003 December spectrum contained a series of Ti I lines with inverse P Cygni profiles. This is clear evidence that some material is falling inward towards the star.

**Key words:** stars: individual: V838 Mon

## 1 INTRODUCTION

The multiple outburst episode of V838 Mon in early 2002 has been well documented (Munari et al. 2002; Kimeswenger et al. 2002; Crause et al. 2003; Banerjee & Ashok 2002; Wisniewski et al. 2003; Rushton et al. 2005). The object was first detected in outburst on 2002 January 6 ( $V_{\max} = 10$ ) (Brown et al. 2002), and subsequent outbursts developed in 2002 February ( $V_{\max} = 6.7$ ) and 2002 March ( $V_{\max} = 7$ ). Optical spectroscopy showed a cool, reddened object, whose continuum shape and absorption spectrum were broadly consistent with those of a K supergiant. However, many of the spectral lines displayed P Cygni profiles, indicating outflow speeds of  $\sim 200 \text{ km s}^{-1}$ , and exhibited strong variability. The post-eruption phase was characterised by a dramatic increase in  $V - I$ , accompanied by a rapid trend towards later spectral types. As of 2002 May the visual magnitude had faded by  $\sim 7$  mag since the 2002 March peak, and the effective temperature was 2400 K (Banerjee & Ashok 2002). By 2002 September further bolometric fading had revealed the presence of a possible B3 V companion (Desidera & Munari 2002). At this time the near-infrared spectrum of V838 Mon displayed very deep H<sub>2</sub>O, CO, TiO, VO and AlO bands, and superficially resembled L-type brown dwarfs, indicating a very cool giant/supergiant (Evans et al. 2003).

V838 Mon may not be a unique object. The similarities with V4332 Sgr and M31 RV are broad-based (Munari et al. 2002; Kimeswenger et al. 2002; Boschi & Munari 2004), and a further analogue may be found in the ‘‘Peculiar Variable in Crux’’ (Della Valle, Saviane & Wenderoth 2003). Recently Banerjee et al. (2003) presented a near-infrared spec-

trum of V4332 Sgr, which also displayed strong AlO bands, but in emission. Accretion models involving stellar mergers (Soker & Tylanda 2003) and planets (Retter & Marom 2003) have been proposed to collectively explain this group of unusual objects.

Here we present some of our latest observations of the near-infrared monitoring program of V838 Mon, emphasizing the discovery of SiO overtone emission and inverse P-Cygni profiles on some atomic lines.

## 2 OBSERVATIONS

Low and high resolution infrared spectroscopy of V838 Mon were obtained on numerous occasions between late 2002 and end 2003, using the facility instrument CGS4 (Mountain et al. 1990) on the United Kingdom Infrared Telescope (UKIRT). An observing log for the specific observations presented here from that time interval is provided in Table 1; additional spectra obtained during that period will be reported later. The observations employed the CGS4 40 l/mm and echelle gratings at resolving powers of  $\sim 1400$  and 20,000 respectively. Flux calibration and removal of telluric absorption features were achieved by dividing the target spectra by spectra of nearby calibration stars. To avoid spurious emission lines in the ratioed spectra due to hydrogen absorption lines in the calibration stars, the Pa $\beta$ , Pf $\gamma$  and Br $\alpha$  lines were removed from the calibration stars by interpolation prior to ratioing. The low resolution ratioed spectra were then multiplied by a blackbody corresponding to the effective temperature and broadband photometric magnitudes of the standard star to give the fi-

**Table 1.** Observing log.

Observation date (UT)	Wavelength coverage ( $\mu\text{m}$ )	Resolving Power	Std. Star
2002 December 17	2.9–4.1	1400	BS2530 (F2 V)
2003 April 4	2.9–4.1	1400	BS2530 (F2 V)
2003 October 6	2.9–4.1	1400	BS2530 (F2 V)
2003 December 6	1.278–1.286	20,000	BS1879 (O8 III)
2003 December 6	3.989–4.021	20,000	BS1879 (O8 III)
2003 December 17	4.016–4.046	20,000	BS1879 (O8 III)

nal flux-calibrated spectra. The high resolution spectra were scaled to make the continuum equal to unity after division. At low resolution, wavelength calibration was carried out by obtaining argon lamp spectra immediately before the target and is accurate to better than  $0.001 \mu\text{m}$ . Argon lines also were used to calibrate the echelle spectrum at  $1.28 \mu\text{m}$ , but telluric  $\text{N}_2\text{O}$  absorption lines in the spectrum of the calibration star were used to calibrate the  $4 \mu\text{m}$  echelle spectra, in both cases to an accuracy of  $\pm 3 \text{ km s}^{-1}$ .

### 3 THE OH AND SiO BANDS

The spectral evolution of V838 Mon (2002 December–2003 October) in the range  $2.9\text{--}4.1 \mu\text{m}$  is shown in Figure 1. The bulk of the detail in the  $2.9\text{--}3.5 \mu\text{m}$  region is due to a combination of the  $\nu_1$  and  $\nu_3$  stretching bands of  $\text{H}_2\text{O}$ . We have observed strong water bands in V838 Mon previously in *JHK* spectroscopy, as discussed in Evans et al. (2003).

The OH fundamental ( $\Delta\nu = 1$ ) *P* branch lines straddle this wavelength range in late-type, O-rich stars. The line positions of the  $\nu = 1 \rightarrow 0$  band, obtained from Maillard, Chauville & Mantz (1976) are indicated in the Figure. The line strengths are usually slowly varying across the band, as the excitation energy varies slowly as a function of  $J$ . The  $P(19) - P(23)$  lines are the only OH lines present in the spectra and their intensities clearly fade over the period of our observations. The lack of higher excitation OH emission lines can be ascribed to temperature, but it is difficult to account for features at lower  $J$  unless OH absorption, increasing towards lower  $J$ , is also present. Higher resolution observations might reveal such absorption. OH transitions involving higher vibrational states do not appear to contribute significantly in this wavelength range.

The SiO first overtone ( $\Delta\nu = 2$ ) is conspicuous in the  $\lambda \gtrsim 4 \mu\text{m}$  region in emission, as was reported by Lynch et al. (2004). In all of our spectra the  $\nu = 2 \rightarrow 0$  band is clearly visible, but there is little or no evidence for the  $\nu = 3 \rightarrow 1$  bandhead. Therefore only the lowest vibrational states  $\nu \lesssim 2$  are significantly populated.

To produce a significant population in the  $\nu = 2$  level by collisional excitation from  $\nu = 1$  the density must be  $\gtrsim A_{10}/C_{12}$ , where  $A_{10}$  is the Einstein coefficient for spontaneous decay from  $\nu = 1$  to  $\nu = 0$ . For SiO- $\text{H}_2$  collisions we can estimate the rate constant  $C_{12}$  for collisional excitation from the  $\nu = 1$  to the  $\nu = 2$  level using the vibrational relaxation time formula given in Millikan & White (1963). Assuming, as is usual (Scoville et al. 1980), the de-excitation cross sections scale like the radiative matrix elements, and using detailed balance, we obtain  $C_{12} \simeq 5.6 \times 10^{-13} \text{ cm}^{-3}$ .

The required density is then  $n_{\text{H}_2} \gtrsim 9.2 \times 10^{12} \text{ cm}^{-3}$  at the excitation temperature of the SiO (see below). This will be an overestimate if there is a significant fractional amount of atomic hydrogen ( $n_{\text{H}} \gtrsim n_{\text{H}_2}/100$ ), since laboratory experiments with CO show that the rate coefficients for collisions with H are  $\sim 100$  times larger than those involving  $\text{H}_2$  (see Scoville et al. 1980 and references therein).

Figure 2 shows a later spectrum at high resolution in the spectral range  $3.98\text{--}4.05 \mu\text{m}$ . This covers portions of the  $\nu = 2 \rightarrow 0$  band of the main isotopomers  $^{28}\text{Si}^{16}\text{O}$  and  $^{29}\text{Si}^{16}\text{O}$ . The fine structure is now resolved and emission in the individual rotational-vibrational lines is clearly apparent; all of the SiO lines in this range are *R* branch transitions. The  $^{28}\text{SiO}$  line positions used in Figure 2 were obtained from Lovas, Maki & Olson (1981); these include the positions of the *R* branch lines extending from  $R(19)$  at  $4.0452 \mu\text{m}$  to the bandhead at  $R(68)$  ( $4.0043 \mu\text{m}$ ). The locations of lines from higher  $J$  values are not shown; the wavelengths of these overlap those of the ascending *R* branch but the lines are undoubtedly much weaker. The radial velocity of the low  $J$  lines is  $+79 \pm 4 \text{ km s}^{-1}$  (heliocentric).

In Figure 2 we present a preliminary attempt to model the SiO emission, using a simple, optically thin and isothermal slab with a Boltzmann population. The transition probabilities of the  $^{28}\text{SiO}$  lines used in the model were calculated using the dipole matrix elements given in Tipping & Chackerian (1981). The less-abundant  $^{29}\text{SiO}$  isotopic species is not included in the model. However, there is no clear evidence for its detection in this complex spectrum. The  $^{29}\text{SiO}$  bandhead occurs at  $4.029 \mu\text{m}$ , and the terrestrial abundance ratio  $^{28}\text{Si}/^{29}\text{Si}$  is  $\sim 20$ . The lack of isolated lines in the spectrum makes it difficult to yield a definitive isotopic ratio, and it is only reasonable to conclude  $^{28}\text{Si}/^{29}\text{Si} > 5$  from the present data.

We find that a model with SiO excitation temperatures of  $T \sim 1200 \text{ K}$  is the best representation of the observed spectrum (a more detailed analysis will be presented elsewhere). This is consistent with the low temperatures seen elsewhere in the infrared spectrum (Evans et al. 2003), and suggests the SiO must be located close to the stellar photosphere, rather than further out in the extended atmosphere. However, a lower SiO excitation temperature of  $790 \text{ K}$  was found by Lynch et al. (2004) from their earlier spectra (2003 January and February). Our low resolution data clearly show the SiO emission varying over the twelve months to 2003 December (see Figure 2), with the strongest emission in the 2003 April spectrum, and it is just as pronounced in the Lynch et al. spectra, albeit at a lower resolution (see their Figure 8). A comparison of their results with our 2002 De-

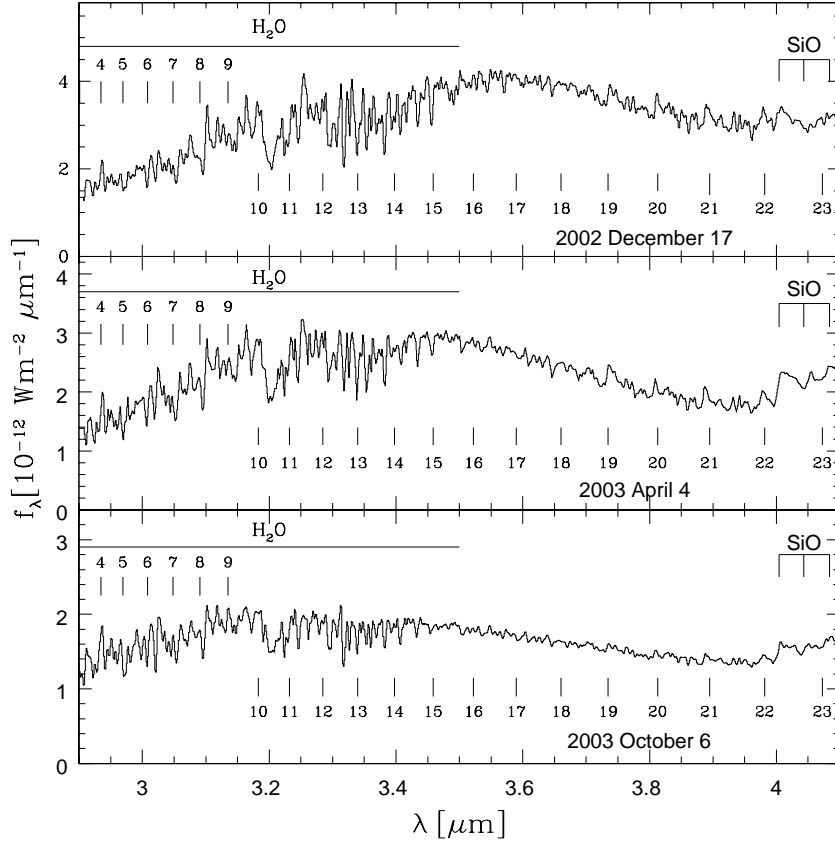


**Figure 1.**  $LL'$  band spectra of V838 Mon on the dates indicated. The vertical lines denote the positions of the OH fundamental transitions shown with their corresponding  $J$  values. The wavelengths of the SiO  $v = 2 \rightarrow 0$ ,  $3 \rightarrow 1$  and  $4 \rightarrow 2$  bandheads are also shown.

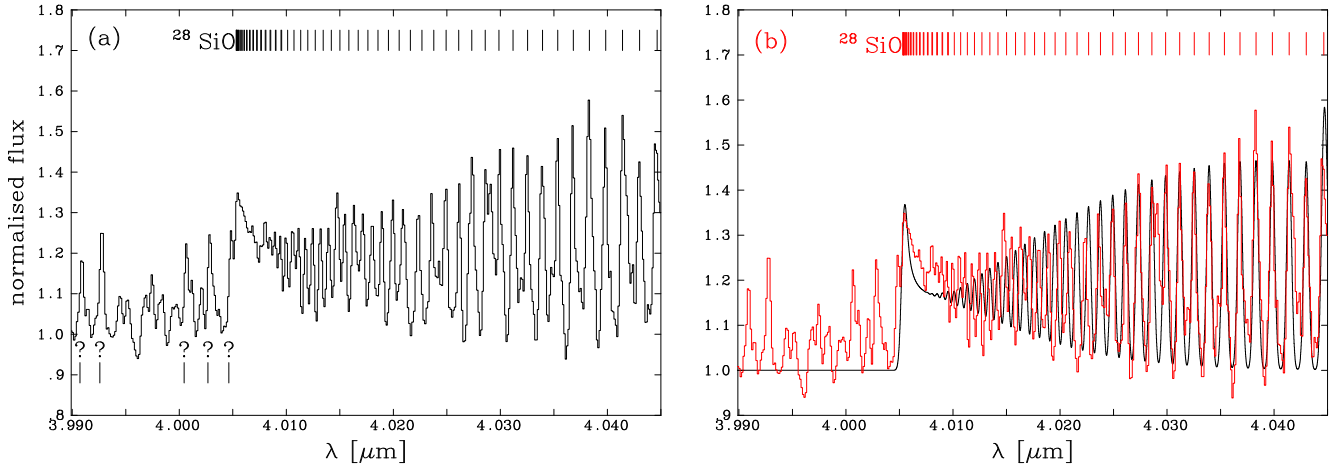


**Figure 2.** (a) 2003 December high resolution spectrum of V838 Mon showing the SiO first overtone emission. The figure also shows five unidentified emission lines. (b) Best fitting model spectrum computed with an excitation temperature of  $T = 1200$  K, superposed on the observed spectrum. The positions of the  $^{28}\text{SiO } v = 2 \rightarrow 0$   $R$  branch lines, redshifted so they occur at  $+79 \text{ km s}^{-1}$  (heliocentric), are indicated in each panel (see text for details).

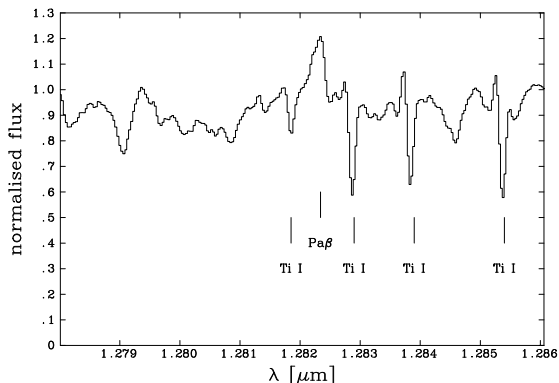


**Figure 3.** A high resolution spectrum of V838 Mon in the region of Pa $\beta$  on 2003 December 6.

ember 17 spectrum, suggests that the flux in the  $\nu = 2 \rightarrow 0$  band had increased by  $\sim 2.5$  times during the following three weeks.

We note that our model spectrum does not match the observed spectrum at a number of wavelengths in the SiO band. This is almost certainly due to the presence of other, as yet unidentified, lines. Five strong unidentified emission lines can be seen in the region shortward of the SiO band head; their observed wavelengths are 3.9907, 3.9926, 4.0003, 4.0026 and 4.0048  $\mu\text{m}$ . It is probable that other such lines overlap the SiO band.

#### 4 EVIDENCE OF INFALL

Figure 3 shows the high resolution spectrum obtained in the wavelength interval 1.278–1.286  $\mu\text{m}$ . Clearly visible are a sequence of three spectral lines bearing well-defined inverse P Cygni profiles with their absorptions centered at 1.2829, 1.2838 and 1.2854  $\mu\text{m}$ . The only spectral features which can possibly account for these lines are the permitted transitions of Ti I at 1.282512, 1.283495 and 1.285054  $\mu\text{m}$ . These resolved Ti I lines are all remarkably narrow, with an average deconvolved FWHM of  $27 \pm 4 \text{ km s}^{-1}$ . The cores of the absorptions occur at a heliocentric radial velocity of  $+88 \pm 7 \text{ km s}^{-1}$ ; the peaks of the emission components are located at  $+65 \pm 6 \text{ km s}^{-1}$ . All of these Ti I lines originate from the b3–z3fo excited states (van Hoof 2004). The excitation energies of the b3 lower levels lie between 1.43 and 1.46 eV above the ground state, and thus could be collisionally excited in a low temperature gas. There is a further Ti I line (1.28115  $\mu\text{m}$ ) present in this spectral region at an observed wavelength of 1.28185  $\mu\text{m}$ , but the lower level of this a3D–y3fo transition is further above the ground state (2.16 eV). This line is in absorption, but may also possess a weak emission component. It is difficult to identify the continuum level in this spectral region.

#### 5 HYDROGEN EMISSION

A notable feature of several low resolution  $J$  band spectra of V838 Mon that we have obtained has been the presence of an emission feature near 1.28  $\mu\text{m}$  (Evans et al. 2003). This

feature is present in the high resolution spectrum shown in Figure 3. The most logical identification for it is Pa $\beta$  (1.282159  $\mu\text{m}$ ). This identification has not been confirmed by detection of other lines. Pa $\alpha$  (1.875613  $\mu\text{m}$ ) occurs in a region of heavy H<sub>2</sub>O blanketing in the star and strong attenuation by telluric H<sub>2</sub>O. Pa $\gamma$  was also not seen in the low resolution data and was not expected given the weakness of the Pa $\beta$  emission. Br $\alpha$ , another expectedly weaker hydrogen line, is not apparent in the low resolution data presented here in Figure 1.

The Pa $\beta$  line peaks at a heliocentric radial velocity of  $+56 \pm 9 \text{ km s}^{-1}$ . The red wing of the emission is almost absent. This is a signature of an accelerating/decelerating flow (Böhm-Vitense & Querci 1987), but the superposition of other spectral features could also account for the asymmetric profile. Pa $\beta$  absorption, redshifted by  $+96 \pm 6 \text{ km s}^{-1}$  (heliocentric), is a possible explanation.

#### 6 DISCUSSION

We have presented infrared observations of V838 Mon which show SiO overtone emission, Pa $\beta$  emission and Ti I lines with inverse P Cygni profiles.

There have not been many reported occurrences of SiO overtone emission in astronomical objects. Of the few known instances, the phenomenon has been observed in SN 1987A (Meikle et al. 1993), the Mira variable, *o* Ceti (Yamamura et al. 1999), the RV Tauri star, R Sct (Matsuura et al. 2002), and is suspected in the latest M giant stars.

The observed SiO bandheads and band structure of the M giant stars SW Vir and RX Boo have been shown to be too weak as compared with the predictions by model atmospheres with appropriate effective temperatures (Tsuji et al. 1994). Similar results were noted by Rinsland & Wing (1982) and Tsuji et al. (1997), who suggest that SiO emission occurs in the outer atmospheres of the coolest O-rich giants, and fills in the strong photospheric SiO absorption lines.

The presence of inverse P Cygni profiles in the post-eruption spectra of V838 Mon is clear evidence that some of the expelled material is now falling toward the star. The presence of SiO and Pa $\beta$  emission can be understood if this infall is being compressed and shock-heated by material close to the star, where there are the high densities necessary to collisionally excite the SiO (see §3). This is similar to the phenomenon seen in pulsating variables where rising and falling layers lead to repetitive shock and line emission very close to the photosphere (Matsuura et al. 2002; Ferlet & Gillet 1984; Gillet et al. 1989).

The SiO emission is redshifted by the same velocity as the Ti I absorption and, if present, the Pa $\beta$  absorption. We therefore conclude that these atomic features must (like the SiO) arise very close to the star. The velocity shifts displayed by the Ti I and Pa $\beta$  emissions are similar. The simplest explanation is that Ti I and Pa $\beta$  trace the same material, with a spherically symmetric distribution, but the difference in excitation suggests that Pa $\beta$  arises in a deeper layer. Our present observations do not allow us to determine whether additional velocity components are present in the SiO emission.

Knowledge of the stellar velocity is required in order to convert our measured velocities to the rest frame of the star. This parameter is uncertain due to the presence of spectral lines with P Cygni profiles in the outburst spectra, and the non-detection of molecular rotational emission (Rushton et al. 2003). Nonetheless Kipper et al. (2004) suggested that the systemic velocity could be  $+59 \pm 6 \text{ km s}^{-1}$  on the basis of two such velocity components in the P Cygni emissions in the outburst spectra. *If* this is the stellar velocity then the infall velocity is  $\sim 15 \text{ km s}^{-1}$ , but again we emphasize the uncertainty in the systemic velocity. The many different outflow velocities and components displayed by the spectral features in the outburst spectra demonstrated the complexities of the gas motions in V838 Mon at that time.

Titanium is the only atomic species with transitions involving low-lying states in the high resolution spectral range presented here. Follow-up observations are necessary to search for infall signatures in other regions of the spectrum, and to monitor the effect of this infall on the future behaviour of V838 Mon.

## ACKNOWLEDGEMENTS

We thank the referee, Geoff Clayton, for his helpful comments. MTR is supported by a Particle Physics and Astronomy Research Council (PPARC) studentship. TRG is supported by the Gemini Observatory, which is operated by the Association of Universities for Research in Astronomy, Inc., on behalf of the international Gemini partnership of Argentina, Australia, Brazil, Canada, Chile, the United Kingdom, and the United States of America.

## REFERENCES

- Banerjee D. P. K., Ashok N. M. 2002, *A&A*, 395, 161  
 Banerjee D. P. K., Varricatt W. P., Ashok N. M., Launila O. 2003, *ApJL*, 598, 31  
 Böhm-Vitense E., Querci M. 1987, in: Kondo Y. (ed.) *Exploring the universe with the IUE satellite*. Kluwer, Dordrecht, p. 223  
 Boschi F., Munari U. 2004, *astro-ph/0402313*  
 Brown N. J., Waagen E. O., Scovill C., Nelson P., Oksanen A., Solonen J., Price A. 2002, *IAUC* 7785  
 Crause L. A., Lawson W. A., Kilkenny D., van Wyk F., Marang F., Jones A. F., 2003, *MNRAS*, 341, 785  
 Desidera S., Munari U., 2002, *IAUC* 7982  
 Della Valle M., Saviane I., Wenderoth E. 2003, *IAUC* 8185  
 Evans A., Geballe T. R., Rushton M. T., Smalley B., van Loon J. Th., Eyres S. P. S., Tyne V. H. 2003, *MNRAS*, 343, 1054  
 Ferlet R., Gillet D. 1984, *A&A*, 133, L1  
 Gillet D., Duquennoy A., Bouchet P., Gouiffes C. 1989, *A&A*, 215, 316  
 Kimeswenger S., Lederle C., Schmeja S., Armsdorfer B. 2002, *MNRAS*, 336, 43  
 Kipper T., Klochkova V. G., Annuk K., Hirv A., Kolka I., Leedjärv L., Puss A., Skoda P., Slechta M. 2004, *A&A*, 416, 1107  
 B.,  
 Lovas F. J., Maki A. G., Olson W. B. 1981, *J. Mol. Spectrosc.*, 87, 449  
 Lynch D. K., Rudy R. J., Russell R. W., Mazuk S., Venturini C. C., Dimpfl W., Bernstein L. S., Sitko M. L., Fajardo-Acosta S., Tokunaga A., Knacke R., Puetter R. C., Perry R. B. 2004, *ApJ*, 607, 460  
 Maillard J., Chauville J., Mantz A. 1976, *J. Molec. Spectrosc.*, 63, 120  
 Matsuura, M., Yamamura, I., Zijlstra, A. A., Bedding, T. R. 2002, *A&A*, 387, 1022  
 Meikle W. P. S., Spyromilio J., Allen D. A., Varani G.-F., Cumming R. J. 1993, *MNRAS*, 261, 535  
 Millikan R. C., White D. R. 1963, *J. Chem. Phys.*, 39, 3209  
 Mountain C. M., Robertson D. J., Lee T. J., Wade R. 1990, *Proc. SPIE*, 1235, 25  
 Munari U., Henden A., Kiyota S., Laney D., Marang F., Zwitter T., Corradi R. L. M., Desidera S., Marrese P. M., Giro E., Boschi F., Schwartz M. B., 2002, *A&A*, 389, L51  
 Retter A., Marom A. 2003, *MNRAS*, 345, L25  
 Rinsland C. P., Wing R. F. 1982, *ApJ*, 262, 201  
 Rushton M. T., Coulson I. M., Evans A., Nyman L.-Å., Smalley, B., Geballe T. R., van Loon J. Th., Eyres S. P. S., Tyne V. H. 2003, *A&A*, 412, 767  
 Rushton M. T., Geballe T. R., Filippenko A., Chornock R., Li W., Leonard D., Evans A., Smalley B., van Loon J. Th., Eyres S. P. S. 2005, *MNRAS*, Submitted  
 Scoville N. Z., Krotkov R., Wang D. 1980, *ApJ*, 240, 929  
 Soker N., Tylenda R. 2003, *ApJ*, 582, 105  
 Tipping R. H., Chackerian C. 1981, *J. Mol. Spectrosc.*, 88, 352  
 Tsuji T., Ohnaka K., Aoki W., Yamamura I. 1997, *A&A*, 320, L1  
 Tsuji T., Ohnaka K., Hinkle K. H., Ridgway S. T. 1994, *A&A*, 289, 469  
 van Hoof P. 2004, <http://www.pa.uky.edu/~peter/atomic/>  
 Wisniewski J. P., Morrison N. D., Bjorkman K. S., Miroshnichenko A. S., Gault A. C., Hoffman J. L., Meade M. R., Nett J. M. 2003, *ApJ*, 588, 486  
 Yamamura I., de Jong T., Cami, J. 1999, *A&A*, 348, L55

This paper has been typeset from a  $\text{\TeX}/\text{\LaTeX}$  file prepared by the author.